Jurnal Teknokes
Homepage: teknokes.org; Vol. 19, No. 2, pp. 110-122, June 2026;

e-ISSN: 2407-8964
p-ISSN: 1907-7904

RESEARCH PAPER

OPEN ACCES

Effect of phantom orientation angle on antenna sensor response in agar-based homogeneous phantom for abnormal breast tissue detection

Rachma Cherlly Pramata[1], Irmayatul Hikmah[2], Muntaqo Alfin Amanaf[2] and Nur Afifah Zen[2]

[1] Department of Biomedical Engineering, Telkom University, Purwokerto, Indonesia.
[2] Department of Telecommunication Engineering, Telkom University, Purwokerto, Indonesia.

ABSTRACT

Breast cancer remains a major global health concern; therefore, early detection plays a crucial role in reducing its mortality rates. Conventional imaging techniques, such as mammography, have limitations including ionizing radiation exposure and reduced sensitivity in dense breast tissues. Microwave-based sensing has emerged as a promising alternative due to its non-ionizing nature, relatively low cost, and sensitivity to dielectric property contrasts between normal and malignant tissues. This study aims to investigate the effect of phantom orientation angle on the response of an antenna-based microwave sensor for abnormal breast tissue detection. An agar-based homogeneous breast phantom is utilized, with tumor inclusion modeled as regions of different dielectric properties. Measurements are conducted using a Vector Network Analyzer (VNA) over a frequency range of 2–6 GHz, with four orientation angles (0°, 90°, 180°, and 270°). The reflection coefficient (S11) is analyzed to observe variations in electromagnetic response under different conditions. The results indicate that tumor presence causes measurable shifts in resonance frequency and variations in the reflection coefficient (S11). Larger tumors produce greater frequency shifts due to higher dielectric contrast. Furthermore, the orientation angle significantly affects detection sensitivity, which is attributed to the antenna radiation pattern and spatial interaction between electromagnetic waves and the phantom. In conclusion, this study demonstrates that both tumor size and phantom orientation influence antenna sensor response. The novelty of this work lies in the incorporation of orientation-based analysis, providing new insight into spatial electromagnetic interactions and enhancing the potential of microwave sensing systems for accurate and non-invasive breast cancer detection.

PAPER HISTORY

Received April 8, 2026
Revised May 2, 2026
Accepted May 18, 2026
Published June 12, 2026

KEYWORDS

Microwave sensing;
Breast phantom;
Antenna sensor;
Resonance frequency shift;
Reflection coefficient (S11)

CONTACT:

rachmapramata@gmail.com
Irmayatulh@telkomuniversity.ac.id
Nurafifahzen@telkomuniversity.ac.id

I. INTRODUCTION

Finding breast issues early is very important because it helps people get better outcomes and live better lives [1]. Traditional methods, such as mammography, are dependable but have some issues. They use ionizing radiation, which can be a concern, and they can be uncomfortable for patients. Also, how well they work can change depending on how dense the breast tissue is [2][3][4]. These limitations have driven the development of microwave-based non-invasive sensing, which uses the shift in return loss of the phantom to distinguish between normal and abnormal tissue, serving as a first step toward a safe and cost-effective comprehensive imaging system. Microwave methods detect differences in how healthy and unhealthy breast tissues respond to electricity, especially in the gigahertz range of frequencies [5]. Abnormal tissues, such as tumors, which tend to have higher water content and vascularity, exhibit greater dielectric constant and conductivity than surrounding normal tissue [6]. The dielectric contrast between healthy and abnormal tissue is what microwaves detect. This physical characteristic allows microwaves to identify abnormal tissue, thus becoming the basic principle for abnormal tissue detection techniques [7].

This study utilized a homogeneous material-based phantom as a representation of breast tissue, which is varied in simulating normal conditions (fat), small tumors, and large tumors, in order to create well-managed biological conditions [8][9]. Return Loss (Parameter S11), as one of the scattering indicators in the S-parameter group, is a key tool for evaluating the performance of antennas and microwave circuits. This measure reflects the degree of impedance matching between the antenna and the transmission line, or the proportion of energy reflected back. In biomedical applications, modifications in the S11 value and resonance point often indicate changes in the environment surrounding the antenna, such as the appearance of diseased tissue [10][11]. The greater the mismatch caused by the tumor, the higher the S11 value (closer to 0 dB) and the greater the observed

Corresponding author: Rachma Cherlly Pramata, rachmapramata@gmail.com, Department of Biomedical Engineering, Telkom University, Purwokerto, Indonesia, Jl. D.I. Panjaitan No. 128, Purwokerto, 53147, Jawa Tengah, Indonesia.
DOI: https://doi.org/10.35882/jteknokes.v19i2.160

e-ISSN: 2407-8964
p-ISSN: 1907-7904

shift in resonance frequency. Previous studies have demonstrated the potential of the S11 parameter for identifying abnormal tissue [12]. However, the effects of the orientation of the abnormal tissue relative to the antenna and the S11 variation patterns at different angles still require further exploration for system optimization. A comprehensive understanding of the antenna's interaction with abnormal tissue at various positions and sizes is crucial for the innovation of a reliable and accurate detector [13][14].

Despite these advancements, most existing studies primarily focus on dielectric contrast without systematically considering the effect of target orientation relative to the antenna. In realistic scenarios, the position and orientation of anomalies are not fixed, which may significantly influence electromagnetic interactions and detection sensitivity. Furthermore, although approaches such as microwave imaging and antenna-based sensing have been widely investigated, the influence of object orientation on antenna response has not been thoroughly analyzed. This indicates a research gap in understanding how spatial orientation affects electromagnetic field distribution and system performance. Based on this gap, this study proposed the hypothesis that the orientation of the phantom significantly affects the electromagnetic interaction and consequently influences the S11 response and resonance frequency shift.

This study further proposed a methodical examination of the S11 response of microwave antennas to abnormal tissue in a homogeneous agar-based phantom representing the breast. The methodology includes testing normal (fat), small tumor, and large tumor conditions, with varying phantom orientations (0°, 90°, 180°, and 270°) to analyze directional sensitivity. The analysis focused on the resonance frequency shift pattern and minimum S11 variation to optimize detection. The main objective of this study is to attempt a structured examination of the S11 parameter pattern of a microwave antenna that reacts to tissue abnormalities in a homogeneous phantom based on agar material, with a focus on the differences in phantom angles (0°, 90°, 180°, and 270°) and the scale of small and large tumors. The findings are expected to contribute in-depth understanding for the improvement of microwave sensing systems using antenna sensors that are more reliable in recognizing breast anomalies.

This study yields several important contributions, including 1) a detailed study of the influence of the position of an agar-based homogeneous phantom containing abnormal tissue on the antenna S11 pattern over a range of angles (0°, 90°, 180°, and 270°), 2) mapping the deviation patterns of resonance frequency and minimum S11 due to tumor size variations, 3) offering new insights for orientation-adaptive S11-frequency curve interpretation algorithms, and 4) confirming the effectiveness of using an agar-based homogeneous phantom as a representative model for breast tissue simulation in microwave studies.

The structure of this paper is as follows: section II describes the research methodology, including antenna design, phantom fabrication, and measurement procedures. Section III presents the experimental results, including S11 data for free-space, normal, small tumor, and large tumor conditions at various orientations. Section IV discusses the interpretation of the results and conceptual implications. Finally, Section V summarizes the main findings and outlines future research directions.

II. MATERIALS AND METHOD

A. Homogenous Breast Phantom Fabrication

A homogeneous phantom was created as a representation of breast tissue by adapting the agar-based synthetic material formulation method from Islam et al. (2018) with standard measurements adjusted to fit the mold volume (1:2). In this method, the main ingredients of the phantom consist of distilled water, polyethylene powder, agar, sodium chloride (NaCl), xanthan gum, and sodium dehydroacetate monohydrate as a preservative. In this composition, polyethylene powder is used to manage electrical permittivity, NaCl is responsible for conductivity, and agar alongside xanthan gum helps keep the phantom's structure and viscosity comparable to that of semi-solid biological tissue [14]. Nevertheless, the preservative was changed from sodium dehydroacetate monohydrate to sodium benzoate. This modification aimed to enhance the biological stability and curb microbial growth of the phantom during storage.

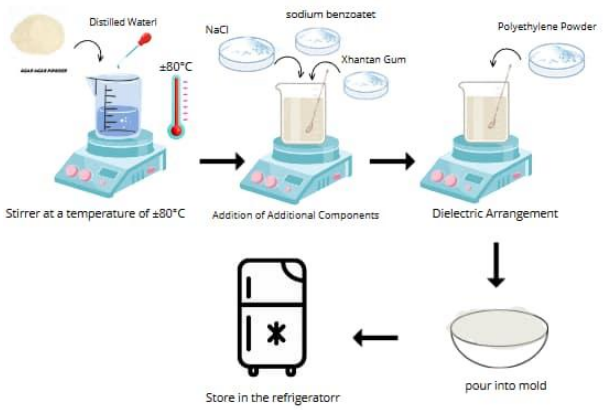

Fig. 1. Fabricated homogenous breast phantom without tumor used in experimental measurement

The use of preservatives in gel-based phantoms is necessary because materials such as agar and gelatin have high-water content, making them prone to biological degradation and microbial growth during storage. If no additives or preservatives are added, agar gel can allow bacteria and fungi to grow, which can damage the phantom material and alter its physical characteristics. Additionally, agar-based phantoms may not stay stable for a long time, which means their properties can change as time passes, possibly influencing the outcomes of

Corresponding author: Rachma Cherlly Pramata, rachmapramata@gmail.com, Department of Biomedical Engineering, Telkom University, Purwokerto, Indonesia, Jl. D.I. Panjaitan No. 128, Purwokerto, 53147, Jawa Tengah, Indonesia.
DOI: https://doi.org/10.35882/jteknokes.v19i2.160

e-ISSN: 2407-8964
p-ISSN: 1907-7904

Table. 1. Composition of materials used in making agar-based homogenous phantoms

Material	Fatty Phantom	Tumor	Purpose
Distilled Water	210 mL	210 mL	Solvent
Polyethylene Powder	250 g	21.5 g	Modifying electrical permitivity
Agar	10 g	10 g	Mechanical strength
Natrium Clorida (NaCl)	1.15 g	14.15 g	Modifying electrical conductivity
Xanthan Gum	3.125 g	3.125 g	Thickener
Sodium Benzoate	0.125 g	0.125 g	Preservative

experiment [15][16]. Some research projects on making tissue-like phantoms have mentioned that sodium benzoate is used in gel phantoms as a preservative. This helps stop bacteria and other microbes from growing and keeps the material's structure stable throughout the experiments. Besides acting as an antimicrobial agent, adding sodium benzoate also helps keep the gel mixture from separating, ensuring that the phantom's mechanical properties and characteristics stay consistent for a longer time [17]. The composition of the homogeneous phantom material is shown in Table 1.

The phantom creation process was carried out in stages

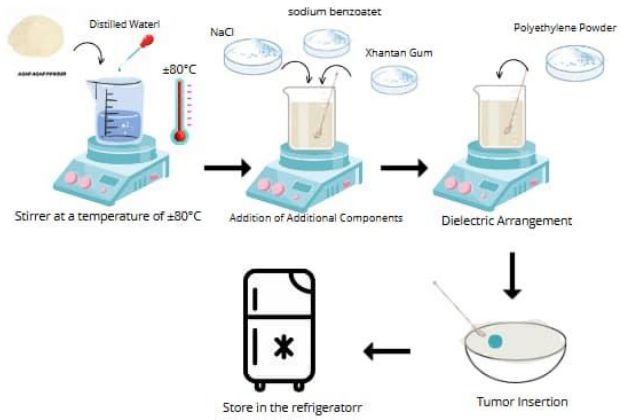

Fig. 2. Fabricated homogenous breast phantom with tumor used in experimental measurement

as shown in Fig. 1. and Fig. 2. First, the agar material was dissolved in distilled water, then NaCl and sodium benzoate were added. The mixture was heated at a temperature of around 80 °C until the solution became homogeneous and transparent

Heating was carried out until bubbles began to appear in the solution, indicating that the mixture has reached a homogeneous state. After the heating process was complete, the solution was transferred to a mixing container. Next, xanthan gum was added to the solution and stirred until evenly mixed. Polyethylene powder was then added gradually while continuing to stir until the mixture was homogeneous. The homogenized phantom mixture was then poured into a cylindrical mold. During the molding process, a spatula was used to create a hollow hole that would be used as a place to insert the tumor material. In this study, the cavity was made with a diameter of 3 cm for small tumors and 6 cm for large tumors. The tumor material was made using the same procedure as the homogeneous phantom, but with a different composition ratio to produce a contrast in dielectric properties compared to normal tissue. After the molding process was complete, the phantom was cooled and left for approximately 24 hours until the material structure was stable before being used in the measurement process shown in Fig. 3.

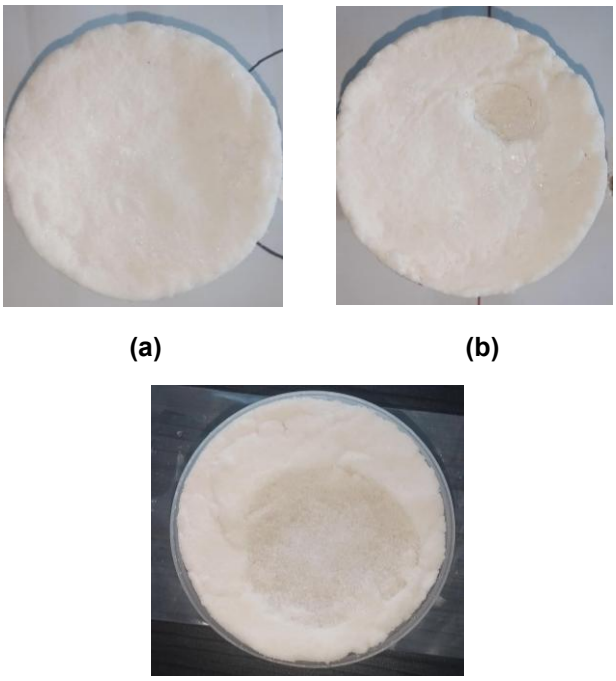

(a) **(b)**

(c)

Fig. 3. Fabricated homogenous breast phantom (a) phantom without tumor (b) phantom with small tumor (c) phantom with large tumor

B. Measurement Setup

Data measurements were performed using an antenna-based sensor system connected to a Vector Network Analyzer (VNA) to measure electromagnetic reflection parameters, as shown in Fig. 4. The antenna was positioned at a fixed position throughout the testing

Corresponding author: Rachma Cherlly Pramata, rachmapramata@gmail.com, Department of Biomedical Engineering, Telkom University, Purwokerto, Indonesia, Jl. D.I. Panjaitan No. 128, Purwokerto, 53147, Jawa Tengah, Indonesia.
DOI: https://doi.org/10.35882/jteknokes.v19i2.160

e-ISSN: 2407-8964
p-ISSN: 1907-7904

process to maintain system configuration consistency. Prior to measurement, the VNA was calibrated using the Short-Open-Load-Through (SOLT) method to minimize

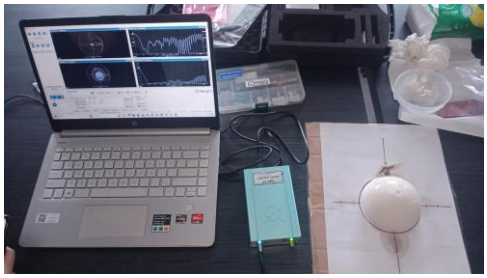

(a)

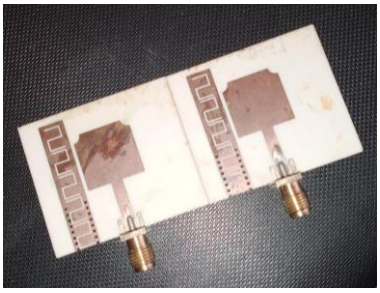

(b)

Fig. 4. Data measurement used~~s~~ an antenna-based sensor system connected to a Vector Network analyzer (VNA) to measure electromagnetic reflection parameters (a) Measurement setup (b) Antenna monopole

systematic errors. The frequency resolution and measurement uncertainty were controlled to ensure reliable data acquisition. The phantom that has been created will be placed in front of the antenna at a constant distance during the measurement process. Testing will be carried out in four conditions, namely free space as the baseline condition, a normal phantom (fatty phantom), a phantom with a small tumor (3 cm diameter), and a phantom with a large tumor (6 cm diameter). To evaluate the effect of orientation on sensor sensitivity, the phantom was rotated at four orientation angles: 0°, 90°, 180°, and 270°. The antenna was not moved during the testing process until the observed changes in electromagnetic response were only caused by changes in the medium conditions and phantom orientation. The observed parameter was the reflection coefficient (S11) recorded in the frequency range of 2–6 GHz using a VNA. This reflection parameter-based measurement approach is commonly used in microwave-based tumor detection research because changes in the dielectric properties of the medium can affect the resonance characteristics of the antenna.

The frequency range of 2–6 GHz was chosen based on the dielectric dispersion characteristics of biological tissue and the relationship between frequency, resolution, and penetration depth of electromagnetic waves. The wavelength in the medium is expressed as **Eq. (1)**:

$$\lambda = \frac{c}{f\sqrt{\varepsilon_r}} \qquad (1)$$

in this context, λ represents the wavelength of the electromagnetic wave, f denotes the operating frequency, and ε_r refers to the relative permittivity of the medium, which characterizes how the material affects the propagation of the wave compared to free space, showing that increasing frequency results in higher resolution. However, the penetration depth of electromagnetic waves is inversely proportional to frequency and can be described by the skin depth parameter δ, which is defined as the distance at which the field amplitude decreases to $1/e$ of its initial value [18]. Mathematically, penetration depth in biological tissue can be expressed as a function of frequency, permittivity, and conductivity of the medium. Furthermore, the interaction of electromagnetic waves with biological tissue is highly frequency-dependent, thus affecting energy distribution and detection sensitivity [19]. Therefore, the 2–6 GHz frequency range was chosen as the optimal compromise between penetration capability and resolution in microwave-based detection systems.

C. Data Processing

Measurements were conducted in stages, starting from free space conditions to obtain system reference values. Next, a normal phantom was placed in the measurement

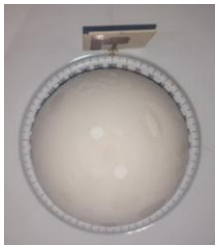

(a)

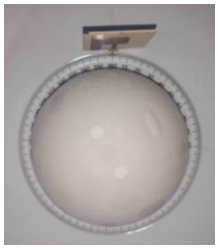

(b)

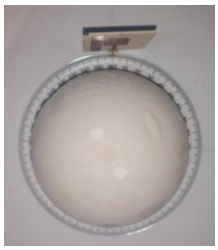

(c)

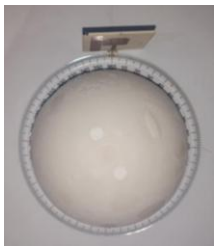

(d)

Fig. 5. The phantom was placed at each orientation angle (a) phantom at 0° angle (b) phantom at 90° angle (c) phantom at 180° angle (d) phantom at 270° angle

conditions and the S11 parameters were recorded over a frequency range of 2-6 GHz. The same procedure was then performed for phantoms with small and large tumors. In each phantom condition, measurements were placed at four angular orientations: 0°, 90°, 180°, and 270° by rotating the phantom relative to the antenna as shown in

Corresponding author: Rachma Cherlly Pramata, rachmapramata@gmail.com, Department of Biomedical Engineering, Telkom University, Purwokerto, Indonesia, Jl. D.I. Panjaitan No. 128, Purwokerto, 53147, Jawa Tengah, Indonesia.
DOI: https://doi.org/10.35882/jteknokes.v19i2.160

Fig. 5. The rotation was performed about the z-axis and can be expressed mathematically using the rotation matrix in **Eq. (2)**:

$$R_z(\theta) = \begin{bmatrix} \cos\theta & -\sin\theta \\ \sin\theta & \cos\theta \end{bmatrix} \quad (2)$$

Where, θ = 0°, 90°, 180°, and 270°. This rotation changed the relative position of the tumor to the antenna radiation pattern, thereby affecting the electromagnetic field distribution and detection sensitivity. Each measurement produced a curve of the relationship between frequency and S11 (dB) values, which was then saved in spreadsheet format for further analysis. Each measurement was repeated at least three times for every condition and orientation. The obtained data were averaged, and standard deviation was calculated to evaluate measurement uncertainty. This approach ensures reproducibility and minimizes the influence of system noise.

D. Data Analysis

The S11 reflection data obtained from the measurements were analyzed to determine the main detection parameters, namely the resonance frequency, the minimum S11 value, and the resonance frequency shift. The resonance frequency was determined as the minimum point on the S11 curve at each phantom condition and angular orientation. The minimum S11 value was also recorded to evaluate changes in the antenna's reflection characteristics due to differences in the dielectric properties of the medium. Furthermore, the S11 curves were compared across phantom conditions and their angular orientations to identify patterns of electromagnetic response changes. The change in resonance frequency (Δf) was used as the primary indicator in detecting the presence and size of anomalies, which was directly related to changes in the effective permittivity of the medium [20]. To increase objectivity and consistency in determining the resonance frequency, the S11 data were analyzed using a curve fitting method. This approach is commonly used in microwave resonator sensor analysis to extract physical parameters from scattering data [21]. Mathematically, the curve $S_{11}(f)$ can be approximated using a second-order polynomial model such as **Eq. (3)**:

$$S_{11}(f) \approx af^2 + bf + c \quad (3)$$

Where $a, b,$ and c are the coefficients resulting from the fitting process. This polynomial approach is widely used in modeling the relationship between resonance parameters and the dielectric properties of materials based on experimental data.

The resonance frequency was then determined by finding the minimum point of the function using the first derivative in **Eq. (4)**:

$$\frac{dS_{11}}{df} = 0 \quad (4)$$

S11 represents the reflection coefficient of the antenna, which indicates how much of the incident signal is reflected back from the antenna, while f denotes the operating frequency. The condition $\frac{dS_{11}}{df} = 0$ signifies that the rate of change of the reflection coefficient with respect to frequency is zero, indicating a stationary point that typically corresponds to the resonant frequency of the antenna.

This approach allows for more stable resonance frequency estimation than direct minimum-finding methods on discrete data, especially in the presence of measurement noise. Furthermore, fitting techniques are widely used in resonance analysis to improve the accuracy of frequency parameter extraction and system characteristics.

E. Theoretical Background

To strengthen the theoretical basis, the interaction between electromagnetic waves and the phantom medium can be explained through Maxwell's equations. In the frequency domain, the relationship between electric and magnetic fields is expressed as **Eq. 5**:

$$\nabla \times \boldsymbol{E} = -j\omega\mu\boldsymbol{H}$$
$$\nabla \times \boldsymbol{H} = (\sigma + j\omega\varepsilon)\boldsymbol{E} \quad (5)$$

In the equations, $\boldsymbol{E}$ is the electric field, $\boldsymbol{H}$ is the magnetic field, $\nabla \times$ denotes the curl operator, j is the imaginary unit, ω is the angular frequency, ε is the electric permittivity, μ is the magnetic permeability, σ and is the electrical conductivity of the medium

Changes in dielectric properties affect the propagation constant as in **Eq. (6)**:

$$\gamma = \sqrt{j\omega\mu(\sigma + j\omega\varepsilon)} \quad (6)$$

This change has a direct impact on the antenna input impedance Z_{in}, which then affects the reflection coefficient (S11) in **Eq. (7)**:

$$S11 = \Gamma = \frac{Z_{in} - Z_0}{Z_{in} + Z_0} \quad (7)$$

Resonance occurs when the matching condition is optimal, that is, when $|S_{11}|$ is minimum. Environmental changes (phantom/tumor) cause changes in Z_{in} thus shifting the resonance frequency. The phantom dielectric properties were modeled as a function of frequency using the Debye model approach in **Eq. (8)** below:

$$\varepsilon(\omega) = \varepsilon_\infty + \frac{\varepsilon_\delta + \varepsilon_\infty}{1 + j\omega\tau} + \frac{\sigma}{j\omega\varepsilon_0} \quad (8)$$

In this context, ε_δ represents the static permittivity, ε_∞ denotes the high-frequency permittivity, and τ is the relaxation time of the medium.

This model explains that increasing the water content in tumors increases permittivity and conductivity, thereby strengthening the wave interactions.

III. RESULTS

A. Reflection Coefficient (S11) Characteristics in Free Space

Initial measurements were conducted in free-space conditions to obtain the antenna's baseline response

Corresponding author: Rachma Cherlly Pramata, rachmapramata@gmail.com, Department of Biomedical Engineering, Telkom University, Purwokerto, Indonesia, Jl. D.I. Panjaitan No. 128, Purwokerto, 53147, Jawa Tengah, Indonesia.
DOI: https://doi.org/10.35882/jteknokes.v19i2.160

e-ISSN: 2407-8964
p-ISSN: 1907-7904

without the influence of the dielectric medium. The measurements showed a resonant frequency of approximately 2.65 GHz with a minimum S11 value of -39.83 dB. This condition represents the unloaded state of the antenna, and therefore serves as a reference for comparing changes occurring in the phantom state. The low minimum S11 value indicates good impedance matching between the antenna and the measurement system.

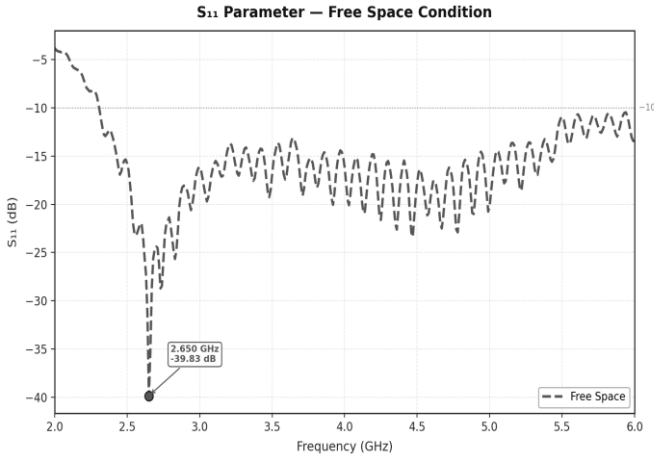

Fig. 6. Measured reflection coefficient (S11) charachteristics of the antenna sensor in free space

Fig. 6. shows a graph of the measured reflection coefficient characteristics (S11) of the antenna sensor in free space, the resonance frequency and the minimum S11.

B. S11 Response of Homogeneous Phantom Without Tumor (Normal)

When a normal phantom was introduced, the resonant frequency shifted to the 2.54–2.58 GHz range. This shift is caused by an increase in the effective permittivity of the medium surrounding the antenna, which affects the input impedance Z_{in} and the reflection coefficient S11. Specifically, at 0°, the resonance occurred at 2.58 GHz with a reflection coefficient of −40.90 dB. At 90° and 180°, the resonant frequency was observed at 2.54 GHz with reflection coefficients of −43.64 dB and −44.69 dB, respectively. Meanwhile, at 270°, the resonance remained at 2.54 GHz with a reflection coefficient of −37.04 dB.Quantitatively, the frequency shift from free space conditions is in the range:

$$\Delta f = f_{res,free} - f_{res,normal} \approx 0.07 - 0.11\ GHz$$

The variation between angles is relatively small, indicating that the homogeneous phantom provides a stable response. However, the difference in S11 values indicates the influence of orientation on the electromagnetic field distribution. Fig. 7. shows a graph of the measured reflection coefficient characteristics (S11) homogenous phantom without tumor, the resonance frequency and the minimum S11

C. S11 Response of Phantom with Small Tumor

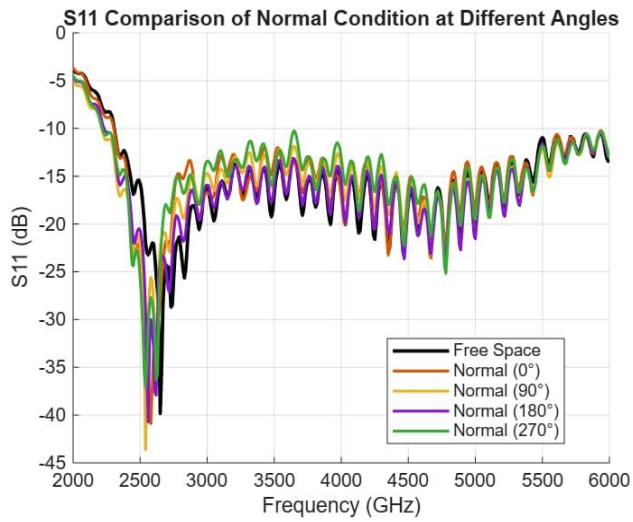

(a)

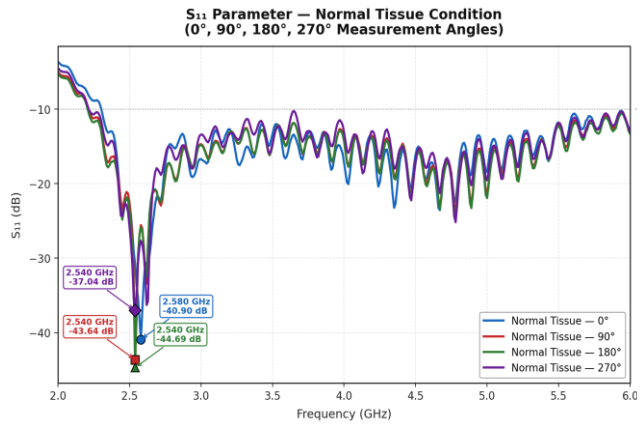

(b)

Fig. 7. (a) Measured reflection coefficient (S11) response of homogenous phantom without tumor, (b) the resonance frequency and the minimum S11.

In the phantom with a small tumor, the resonance frequency ranged from 2.56–2.59 GHz, indicating a relatively small change compared to the normal phantom. This indicates that the small tumor size results in limited dielectric contrast. However, significant changes were observed in the S11 magnitude, particularly at 90° orientation, where the difference between the normal and small tumor conditions reached more than 6 dB. This difference is experimentally larger than the measurement uncertainty and can therefore be considered significant. This finding suggests that small tumor detection is significantly influenced by orientation, which is related to the electromagnetic field distribution around the antenna.

Fig. 8. shows a graph of the measured reflection coefficient characteristics (S11) homogenous phantom with small tumor, the resonance frequency and the minimum S11.

Corresponding author: Rachma Cherlly Pramata, rachmapramata@gmail.com, Department of Biomedical Engineering, Telkom University, Purwokerto, Indonesia, Jl. D.I. Panjaitan No. 128, Purwokerto, 53147, Jawa Tengah, Indonesia.
DOI: https://doi.org/10.35882/jteknokes.v19i2.160

e-ISSN: 2407-8964
p-ISSN: 1907-7904

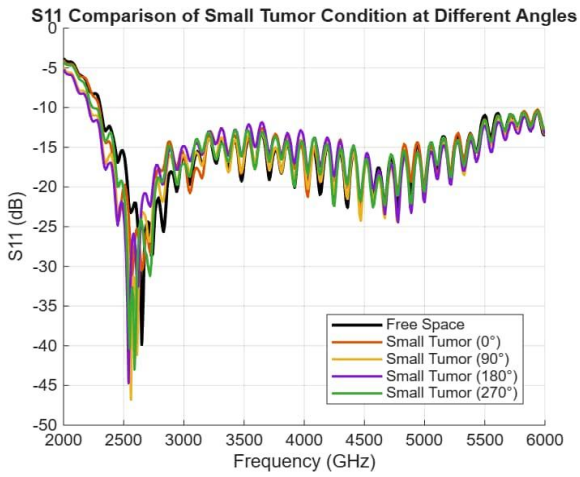

(a)

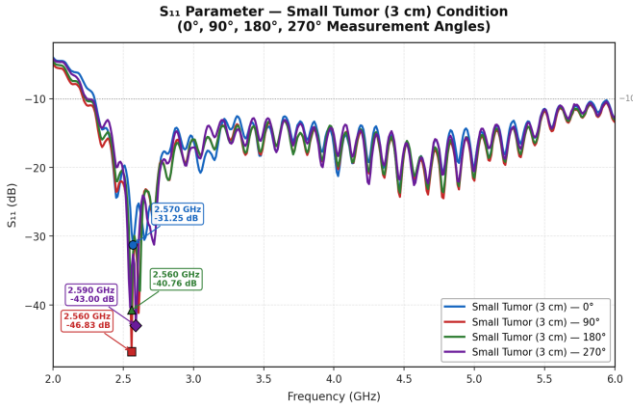

(b)

Fig. 8. (a) Measured reflection coefficient (S11) response of homogenous phantom with small tumor, (b) the resonance frequency and the minimum S11.

D. S11 Response of Phantom with Large Tumor

When a large tumor was introduced, a significant shift in the resonant frequency was observed, ranging from 4.35 to 4.78 GHz. This shift is substantially greater than those observed in the small tumor and normal phantom conditions, with a frequency deviation of approximately $\Delta f \approx 0.07 - 2.1\,GHz$. Specifically, at 0°, the resonance occurred at 4.78 GHz with a reflection coefficient of −22.95 dB. At 90° and 180°, the resonant frequencies were 4.67 GHz and 4.35 GHz, with reflection coefficients of −25.21 dB and −26.67 dB, respectively. Meanwhile, at 270°, the resonance shifted back to 2.62 GHz with a reflection coefficient of −32.36 dB. This substantial frequency shift indicates a strong relationship between tumor size and the dielectric properties of the medium. Larger tumors produce higher dielectric contrast, resulting in more significant electromagnetic field perturbations and consequently more drastic changes in the antenna impedance. However, the observation at 270°, where the resonant frequency returned close to the normal condition, suggests that detection sensitivity is highly dependent on orientation angle. This indicates that suboptimal orientation may reduce detection accuracy, highlighting the importance of spatial configuration in microwave-based breast tumor detection systems Fig. 9. shows a graph of the measured reflection coefficient characteristics (S11) homogenous phantom with large tumor, the resonance frequency and the minimum S11.

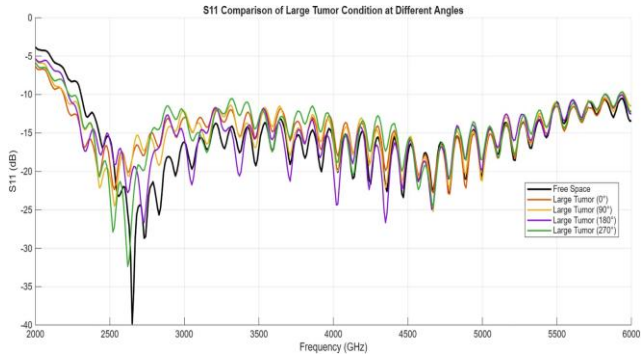

(a)

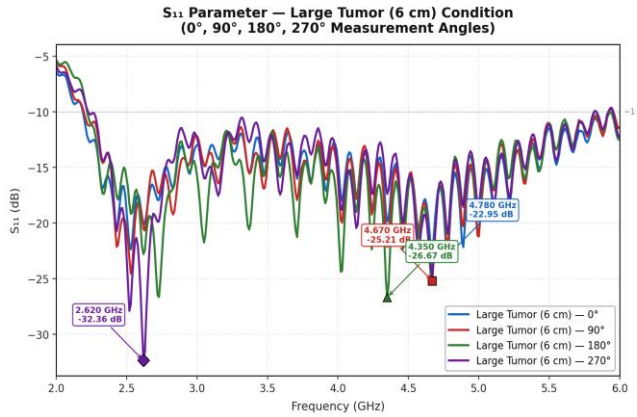

(b)

Fig. 9. (a) Measured reflection coefficient (S11) response of homogenous phantom with large tumor, (b) the resonance frequency and the minimum S11.

E. Effect of Observation Angle on Detection Sensitivity

The analysis of angular variations showed that the 90° and 180° orientations produced the most significant response differences, both in terms of resonance frequency shifts and changes in S11 values. This phenomenon can be explained by the antenna's radiation pattern, where the electromagnetic field distribution is non-isotropic. At certain angles, higher field intensity leads to stronger interactions between the electromagnetic wave and the anomaly, thus increasing detection sensitivity. Conversely, at angles of 0° and 270°, the observed changes were relatively smaller, indicating that the relative position of the antenna and the tumor

Corresponding author: Rachma Cherlly Pramata, rachmapramata@gmail.com, Department of Biomedical Engineering, Telkom University, Purwokerto, Indonesia, Jl. D.I. Panjaitan No. 128, Purwokerto, 53147, Jawa Tengah, Indonesia.
DOI: https://doi.org/10.35882/jteknokes.v19i2.160

e-ISSN: 2407-8964
p-ISSN: 1907-7904

affects detection effectiveness. Fig. 10. shows a graph of the measured reflection coefficient characteristics (S11) homogenous phantom with large tumor, the resonance frequency and the minimum S11.

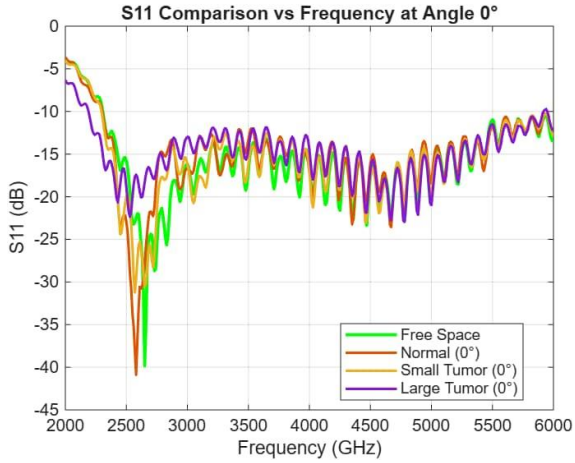

(a)

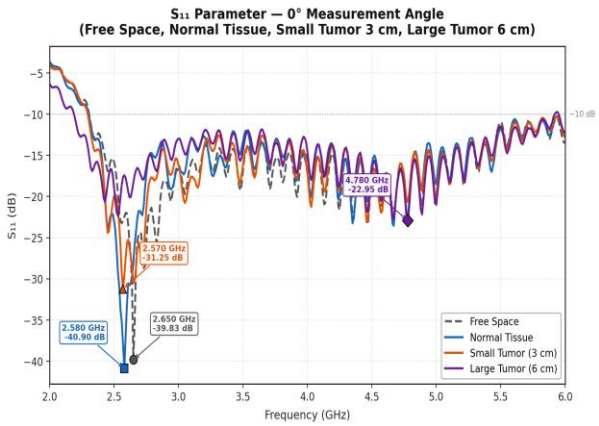

(b)

Fig. 10. (a) Comparison of S11 response for all phantom conditions at 0° orientation, (b) the resonance frequency and the minimum S11.

Fig. 10. shows a graph of the comparison of S11 response for all phantom conditions at 0° orientation, the resonance frequency and the minimum S11.

F. Comparative Analysis of Detection Parameters

Based on all measurement conditions, it can be observed that the detection parameters exhibit different sensitivities depending on the presence and size of the tumor. In the normal condition, both the frequency shift (Δf) and S11 variation were minimal, resulting in low sensitivity. For small tumors, Δf remained relatively small, while changes in S11 became more noticeable, indicating moderate sensitivity. In contrast, large tumors produced a substantial frequency shift along with significant changes in S11, resulting in high detection sensitivity These results indicate that the resonance frequency shift is more sensitive to large dielectric perturbations, making it a reliable indicator for tumor size estimation. On the other hand, variations in the S11 magnitude were more effective for detecting smaller anomalies, particularly in early-stage tumor conditions.

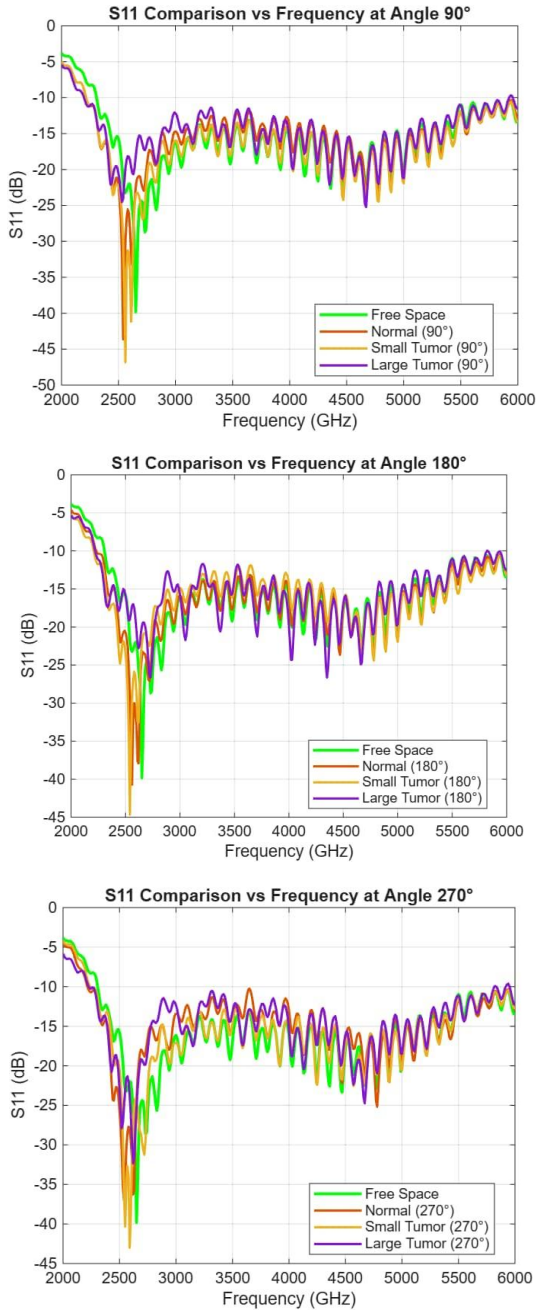

Fig. 11. Comparison of S11 response for all phantom conditions at 90°, 180°, and 270° orientation

Therefore, a combined analysis of both parameters can improve the overall reliability and sensitivity of the detection system, where frequency shift (Δf) serves as an indicator of tumor size, while S11 functions as an indicator of tumor presence. Fig. 12. shows the resonance frequency and the minimum S11 for all phantom

Corresponding author: Rachma Cherlly Pramata, rachmapramata@gmail.com, Department of Biomedical Engineering, Telkom University, Purwokerto, Indonesia, Jl. D.I. Panjaitan No. 128, Purwokerto, 53147, Jawa Tengah, Indonesia.
DOI: https://doi.org/10.35882/jteknokes.v19i2.160

e-ISSN: 2407-8964
p-ISSN: 1907-7904

conditions at 90°, 180°, and 270° orientations.

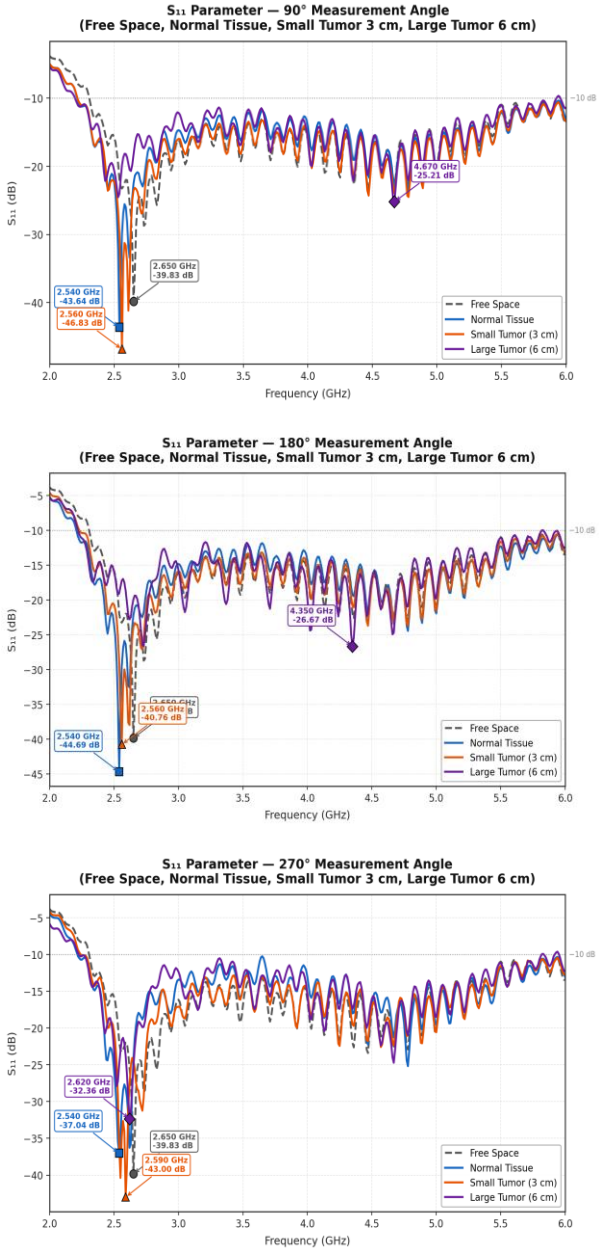

Fig. 12. the resonance frequency and the minimum S11 for all phantom conditions at 90°, 180°, and 270° orientations.

G. Summary of Results

Overall, the resonant frequency decreases in the presence of a normal phantom due to the loading effect, which alters the effective electromagnetic properties surrounding the antenna. In the case of a small tumor, the resonant frequency remains relatively unchanged; however, noticeable variations occur in the magnitude of S11, indicating its sensitivity to small anomalies. In contrast, a large tumor induces a significant frequency shift exceeding 1.7 GHz, reflecting a strong dielectric perturbation within the medium. Furthermore, the orientation angle plays a crucial role in detection sensitivity. The results show that the optimal detection performance is achieved at 90° and 180°, while the 270° orientation demonstrates a potential reduction in detection capability.

IV. DISCUSSION

The results of the study indicate that the presence of the phantom medium and variations in tumor size significantly influence the reflection coefficient (S11) characteristics of the antenna system used. The observed resonance frequency shifts in each condition indicate that the interaction between electromagnetic waves and the phantom material is strongly influenced by differences in dielectric properties between normal and anomalous tissue. This difference in dielectric properties is the basic principle of microwave-based tumor detection methods, where tumor tissue generally has higher permittivity and conductivity than normal tissue due to its higher water content and cell density [22][23].

Under free space conditions, the antenna system exhibited a minimum resonance frequency at 2.65 GHz with an S11 value of −39.83 dB, indicating good impedance matching. When the phantom was introduced, the resonance frequency shifts to a lower range (2.54 GHz-2.58 GHz), which is attributed to the increase in effective permittivity surrounding the antenna. This phenomenon is consistent with electromagnetic theory, where changes in the dielectric environment affect the antenna input impedance (Z_{in}) and consequently modify the reflection coefficient. Similar behavior has been widely reported in resonator-based microwave sensors, where dielectric loading directly alters resonance characteristics [24][25][26].

In the presence of a small tumor, the resonance frequency variation remains relatively limited; however, significant changes were observed in the magnitude of S11, particularly at the 90° orientation. The difference exceeding 6 dB compared to the normal phantom indicates that even small perturbations in dielectric properties can alter the surface current distribution and input impedance of the antenna. This is consistent with microwave resonator theory, where localized changes in dielectric properties modify the electromagnetic field distribution and scattering parameters [27][20]. A more pronounced effect was observed for large tumors, where the resonance frequency shifts significantly up to the range of 4.35–4.78 GHz. This corresponds to a shift exceeding 1.7 GHz relative to the baseline condition, indicating a strong dependence of resonance behavior on tumor size. This trend suggests a proportional relationship between tumor volume and electromagnetic perturbation. In recent studies, resonance frequency has been shown to correlate with dielectric loading and can be predicted or modeled using data-driven or regression-based approaches [25][28][29][30][31]. Therefore, the observed results indicate the potential for developing a semi-empirical model relating frequency shift (Δf) to tumor size.

Corresponding author: Rachma Cherlly Pramata, rachmapramata@gmail.com, Department of Biomedical Engineering, Telkom University, Purwokerto, Indonesia, Jl. D.I. Panjaitan No. 128, Purwokerto, 53147, Jawa Tengah, Indonesia.
DOI: https://doi.org/10.35882/jteknokes.v19i2.160

The analysis of orientation variation reveals that detection sensitivity is highly dependent on the relative position between the antenna and the anomaly. The most significant responses are observed at 90° and 180°, where both resonance frequency shifts and S11 magnitude differences are maximized. This behavior can be explained by the antenna radiation pattern, where the electromagnetic field distribution exhibits directional characteristics, resulting in stronger field–target interactions at specific angles. Similar findings have been reported in microwave resonator-based sensing systems, where the electric field concentration around the resonator determines sensitivity [27].Conversely, at 270°, the resonance frequency for the large tumor condition returns close to the baseline value, indicating a significant reduction in detection sensitivity. This finding is particularly important, as it suggests the possibility of false negative detection when the anomaly is located outside the region of strong electromagnetic field interaction. This limitation has also been highlighted in microwave sensor studies, where field non-uniformity can reduce detection accuracy depending on target position [32][33].

Furthermore, the results demonstrate a clear trend between tumor size and resonance frequency shift. Small tumors produce frequency deviations of less than 0.1 GHz, whereas large tumors result in shifts exceeding 1.7 GHz. This behavior is consistent with microwave sensing principles, where resonance frequency shifts are commonly used to extract material permittivity using curve fitting or empirical modeling approaches. Therefore, resonance frequency can serve not only as a detection parameter but also as a potential quantitative indicator for estimating tumor size [34].Compared to more complex microwave imaging systems, the proposed antenna-based sensing approach offers advantages in terms of simplicity, cost-effectiveness, and ease of implementation. However, the system is more sensitive to orientation, which may limit its robustness in practical applications. Compared to more complex microwave imaging systems, the proposed antenna-based sensing approach offers advantages in terms of simplicity, cost-effectiveness, and ease of implementation. However, the system is more sensitive to orientation, which may limit its robustness in practical applications. This study also has several limitations. The phantom used is homogeneous and does not fully represent the heterogeneous structure of real biological tissues. In addition, experimental validation using clinical data has not yet been conducted. Environmental noise and coupling effects were also not extensively analyzed, which may influence measurement accuracy.

V. CONCLUSION

This study aimed to investigate the effect of phantom orientation angle on the response of an antenna-based microwave sensing system using reflection coefficient (S11) analysis for abnormal breast tissue detection in an agar-based homogeneous phantom. The experimental results demonstrate that the presence of a dielectric medium shifts the resonance frequency from 2.65 GHz (free space) to approximately 2.54–2.58 GHz under normal phantom conditions due to increased effective permittivity. In the case of a small tumor (3 cm), the resonance frequency remains relatively stable within 2.56–2.59 GHz, while a significant change is observed in the S11 magnitude, particularly exceeding 6 dB at certain orientations, indicating sensitivity to small anomalies. In contrast, a large tumor (6 cm) produces a substantial resonance frequency shift up to the range of 4.35–4.78 GHz, corresponding to a deviation greater than 1.7 GHz from the baseline condition. These results confirm that resonance frequency shift is strongly correlated with tumor size, while S11 magnitude variation is more sensitive to smaller anomalies. Furthermore, the orientation angle significantly influences detection performance. The highest sensitivity is achieved at 90° and 180°, where both resonance frequency shifts and S11 differences are maximized. Conversely, at 270°, the resonance response tends to return close to the normal condition, indicating reduced sensitivity and a potential risk of false-negative detection. In conclusion, S11-based microwave sensing provides an effective, low-cost, and practical approach for anomaly detection in biological tissue phantoms. The combined use of resonance frequency shift and S11 magnitude enhances detection capability across different tumor sizes, while orientation-dependent behavior highlights the importance of spatial considerations in system design. For future work, the system can be improved by implementing multi-angle measurement strategies or antenna array configurations to reduce orientation sensitivity. In addition, the use of heterogeneous phantoms that better represent real breast tissue, integration with data-driven or machine learning-based classification methods, and validation using clinical or realistic datasets are recommended to enhance the robustness and applicability of the proposed system for real-world biomedical applications.

REFERENCES

[1] J. M. Seely, “Progress and Remaining Gaps in the Early Detection and Treatment of Breast Cancer,” *Curr. Oncol.*, vol. 30, no. 3, pp. 3201–3205, 2023, doi: 10.3390/curroncol30030242.

[2] Y. X. Lim, Z. L. Lim, P. J. Ho, and J. Li, “Breast Cancer in Asia: Incidence, Mortality, Early Detection, Mammography Programs, and Risk-Based Screening Initiatives,” *Cancers (Basel).*, vol. 14, no. 17, pp. 1–21, 2022, doi: 10.3390/cancers14174218.

[3] C. H. Barrios, “Global challenges in breast cancer detection and treatment,” *Breast*, vol. 62, no. S1, pp. S3–S6, 2022, doi: 10.1016/j.breast.2022.02.003.

[4] A. Bhushan, A. Gonsalves, and J. U. Menon, “Current state of breast cancer diagnosis, treatment, and theranostics,” May 01, 2021, *MDPI*. doi: 10.3390/pharmaceutics13050723.

[5] L. Wang, “Microwave Imaging and Sensing

Corresponding author: Rachma Cherlly Pramata, rachmapramata@gmail.com, Department of Biomedical Engineering, Telkom University, Purwokerto, Indonesia, Jl. D.I. Panjaitan No. 128, Purwokerto, 53147, Jawa Tengah, Indonesia.
DOI: https://doi.org/10.35882/jteknokes.v19i2.160

Techniques for Breast Cancer Detection," *Micromachines*, vol. 14, no. 7, 2023, doi: 10.3390/mi14071462.

[6] F. E. Zerrad *et al.*, "Microwave Imaging Approach for Breast Cancer Detection Using a Tapered Slot Antenna Loaded with Parasitic Components," *Materials (Basel).*, vol. 16, no. 4, 2023, doi: 10.3390/ma16041496.

[7] M. N. Hamza, S. Koziel, and A. Pietrenko-Dabrowska, "Design and experimental validation of a metamaterial-based sensor for microwave imaging in breast, lung, and brain cancer detection," *Sci. Rep.*, vol. 14, no. 1, pp. 1–17, 2024, doi: 10.1038/s41598-024-67103-9.

[8] S. Li, E. Fear, and L. Curiel, "Breast tissue mimicking phantoms for combined ultrasound and microwave imaging," *Phys. Med. Biol.*, vol. 66, no. 24, 2021, doi: 10.1088/1361-6560/ac3d18.

[9] A. Filippou and C. Damianou, "Agar-based Phantom for Evaluating Targeting of High-intensity Focused Ultrasound Systems for Breast Ablation," *J. Med. Phys.*, vol. 49, no. 3, pp. 343–355, 2024, doi: 10.4103/jmp.jmp_52_24.

[10] F. A. ali abdulla and A. Demirkol, "A novel textile-based UWB patch antenna for breast cancer imaging," *Phys. Eng. Sci. Med.*, Sep. 2024, doi: 10.1007/s13246-024-01409-w.

[11] M. Elsaadi and R. Hamad, "Breast Cancer Detection Based on Multi-Slotted Patch Antenna at ISM Band," *Circuits Syst.*, vol. 14, no. 05, pp. 1–9, 2023, doi: 10.4236/cs.2023.145001.

[12] D. Bhargava and P. Rattanadecho, "Microwave imaging of breast cancer: Simulation analysis of SAR and temperature in tumors for different age and type," *Case Stud. Therm. Eng.*, vol. 31, p. 101843, 2022, doi: 10.1016/j.csite.2022.101843.

[13] M. H. Sharaf, M. Arrebola, K. F. A. Hussein, A. E. Farahat, and Á. F. Vaquero, "Conformal On-Body Antenna System Integrated with Deep Learning for Non-Invasive Breast Cancer Detection," *Sensors*, vol. 25, no. 15, pp. 1–37, 2025, doi: 10.3390/s25154670.

[14] M. T. Islam, M. Samsuzzaman, S. Kibria, and M. T. Islam, "Experimental breast phantoms for estimation of breast tumor using microwave imaging systems," *IEEE Access*, vol. 6, pp. 78587–78597, 2018, doi: 10.1109/ACCESS.2018.2885087.

[15] V. Fritz, S. Eisele, P. Martirosian, J. Machann, and F. Schick, "A straightforward procedure to build a non-toxic relaxometry phantom with desired T1 and T2 times at 3T," *Magn. Reson. Mater. Physics, Biol. Med.*, vol. 37, no. 5, pp. 899–907, 2024, doi: 10.1007/s10334-024-01166-7.

[16] G. Menikou and C. Damianou, "Acoustic and thermal characterization of agar based phantoms used for evaluating focused ultrasound exposures," *J. Ther. Ultrasound*, vol. 5, no. 1, pp. 1–14, 2017, doi: 10.1186/s40349-017-0093-z.

[17] S. A. Amiri, P. Van Berckel, M. Lai, J. Dankelman, and B. H. W. Hendriks, "Tissue-mimicking phantom materials with tunable optical properties suitable for assessment of diffuse reflectance spectroscopy during electrosurgery," *Biomed. Opt. Express*, vol. 13, no. 5, p. 2616, 2022, doi: 10.1364/boe.449637.

[18] I. Krimi, S. Ben Mbarek, S. Amara, F. Choubani, and Y. Massoud, "Mathematical Channel Modeling of Electromagnetic Waves in Biological Tissues for Wireless Body Communication," *Electron.*, vol. 12, no. 6, 2023, doi: 10.3390/electronics12061282.

[19] A. Gasmelseed, "Parametric analysis of electromagnetic wave interactions with layered biological tissues for varying frequency, polarization, and fat thickness," *Sci. Rep.*, pp. 1–9, 2025, doi: 10.1038/s41598-025-33460-2.

[20] A. J. A. Al-Gburi, Z. Zakaria, N. Abd Rahman, S. Alam, and M. A. M. Said, "A Compact and Low-Profile Curve-Feed Complementary Split-Ring Resonator Microwave Sensor for Solid Material Detection," *Micromachines*, vol. 14, no. 2, 2023, doi: 10.3390/mi14020384.

[21] R. A. Alahnomi *et al.*, "Review of Recent Microwave Planar Resonator-Based Sensors :," *Sens. Rev.*, vol. 2267, no. 21, pp. 1–38, 2021.

[22] E. G. Fernández-Aranzamendi *et al.*, "Dielectric Characterization of Ex-Vivo Breast Tissues: Differentiation of Tumor Types through Permittivity Measurements," *Cancers (Basel).*, vol. 16, no. 4, 2024, doi: 10.3390/cancers16040793.

[23] Q. Chen *et al.*, "Real-Time Differentiation Between Benign and Malignant Breast Tumors and Other Tissues Using Dielectric Properties," *Med. Sci. Monit.*, vol. 31, 2025, doi: 10.12659/MSM.947531.

[24] M. Särestöniemi, D. Singh, R. Dessai, C. Heredia, S. Myllymäki, and T. Myllylä, "Realistic 3D Phantoms for Validation of Microwave Sensing in Health Monitoring Applications," *Sensors*, vol. 24, no. 6, 2024, doi: 10.3390/s24061975.

[25] M. Bazgir, A. Sheikhi, and M. B. Dowlatshahi, "Resonance frequency prediction of dielectric antennas for liquid sensing via support vector regression," *Sci. Rep.*, vol. 14, no. 1, pp. 1–15, 2024, doi: 10.1038/s41598-024-83069-0.

[26] M. H. Mustafa Kamal, S. A. Qureshi, Z. Zainal Abidin, H. A. Majid, and C. H. See, "Evaluation of microwave square ring metamaterial-based resonator for glucose detection," *J. Eng. Appl. Sci.*, vol. 71, no. 1, pp. 1–16, 2024, doi: 10.1186/s44147-024-00366-1.

[27] M. A. Aldhaeebi and T. S. Almoneef, "Microwave Metasurface-Based Sensor with Artificial Intelligence for Early Breast Tumor Detection," *Micromachines*, vol. 17, no. 2, 2026, doi: 10.3390/mi17020179.

[28] D. M. Elsheakh, S. A. Alsherif, and A. R. Eldamak,

Corresponding author: Rachma Cherlly Pramata, rachmapramata@gmail.com, Department of Biomedical Engineering, Telkom University, Purwokerto, Indonesia, Jl. D.I. Panjaitan No. 128, Purwokerto, 53147, Jawa Tengah, Indonesia.
DOI: https://doi.org/10.35882/jteknokes.v19i2.160

"Textile monopole sensors for breast cancer detection," *Telecommun. Syst.*, vol. 82, no. 3, pp. 363–379, 2023, doi: 10.1007/s11235-023-00990-x.

[29] D. N. Elsheakh, R. A. Mohamed, O. M. Fahmy, K. Ezzat, and A. R. Eldamak, "Complete Breast Cancer Detection and Monitoring System by Using Microwave Textile Based Antenna Sensors," *Biosensors*, vol. 13, no. 1, 2023, doi: 10.3390/bios13010087.

[30] M. N. Hamza, M. T. Islam, and S. Koziel, "Advanced sensor for non-invasive breast cancer and brain cancer diagnosis using antenna array with metamaterial-based AMC," *Eng. Sci. Technol. an Int. J.*, vol. 56, no. July, p. 101779, 2024, doi: 10.1016/j.jestch.2024.101779.

[31] G. Wu *et al.*, "A zirconia-based wideband biological tissue identification probe with enhanced penetration depth," *Front. Phys.*, vol. 13, no. January, pp. 1–12, 2026, doi: 10.3389/fphy.2025.1729565.

[32] H. Song *et al.*, "Detectability of Breast Tumor by a Hand-held Impulse-Radar Detector: Performance Evaluation and Pilot Clinical Study," *Sci. Rep.*, vol. 7, no. 1, 2017, doi: 10.1038/s41598-017-16617-6.

[33] A. R. Celik, "Simulation Measurement for Detection of the Breast Tumors by Using Ultra-Wideband Radar-Based Microwave Technique," *Int. Res. J. Eng. Technol.*, vol. 05, no. 11, pp. 1521–1525, 2018.

[34] L. D'alvia *et al.*, "A Novel Microwave Resonant Sensor for Measuring Cancer Cell Line Aggressiveness," *Sensors*, vol. 22, no. 12, pp. 1–12, 2022, doi: 10.3390/s22124383.

AUTHOR BIOGRAPHY

Rachma Cherlly Pramata is an undergraduate student in the Biomedical Engineering Study Program at Telkom University Purwokerto, Indonesia, since 2022. She is currently in her eighth semester and conducting final year research on detecting abnormal breast tissue using a homogeneous agar-based phantom and an antenna-based microwave sensing system. Her work involves developing phantom materials, performing microwave measurements, and analyzing scattering parameters to identify tissue characteristics. Her research interests include biomedical instrumentation, microwave sensing for medical applications, medical imaging, and biomedical signal analysis, focusing on practical implementation and experimental validation in biomedical engineering research, aiming to contribute to breast cancer detection.

Irmayatul Hikmah received the B.S. degree in Physics from Institut Teknologi Sepuluh Nopember (ITS), Surabaya, Indonesia, in 2015, and the M.Sc. degree in Medical Physics from the same institution in 2019. Since 2019, she has been a Lecturer in the Biomedical Engineering Study Program, Telkom University Purwokerto, Indonesia. She is a member of the Indonesian Alliance of Medical Physicists (AFISMI). Her academic responsibilities include teaching, conducting research, and participating in community engagement programs related to biomedical technology and healthcare applications. Her research focuses on medical physics and biomedical engineering, particularly in radiation dosimetry, medical imaging analysis, biomedical instrumentation, and the application of machine learning techniques for healthcare data analysis. She is also actively involved in interdisciplinary research aimed at developing technology-based solutions to support medical diagnostics, improve healthcare services, and advance the integration of medical physics with biomedical engineering.

Muntaqo Alfin Amanaf received the B.A.Sc. and M.S. degrees in Telecommunication Engineering from Institut Teknologi Sepuluh Nopember (ITS), Surabaya, Indonesia, in 2012 and 2014, respectively. He is currently pursuing a Ph.D. degree in electrical engineering at ITS, Surabaya. Since 2016, he has been a lecturer and assistant professor in the telecommunication engineering study program at Telkom University, Indonesia. His research focuses on wireless communication systems, antenna engineering, and Internet of Things (IoT), particularly the design of microstrip, array, and wideband antennas. His recent work involves compact antenna systems with enhanced isolation and radiation performance for wireless and sensing applications. He has also worked on biomedical antennas for microwave imaging in the early stages of breast cancer detection. His research integrates electromagnetic theory and applied physics to improve signal penetration and imaging accuracy in biological media, contributing to next-generation wireless and biomedical diagnostic systems.

Nur Afifah Zen received B.S. degree in Physics from Universitas Jenderal Soedirman, Indonesia, in 2014, and the M.S. degree in Physics from Institut Teknologi Bandung, Indonesia, in 2018. Since 2018, she has been a lecturer in the Telecommunication Engineering Study Program at Telkom University Purwokerto, Indonesia. Her academic background is strongly rooted in fundamental and applied physics, which serves as the foundation for her interdisciplinary research. Her research interests include advanced functional materials, materials characterization,

Corresponding author: Rachma Cherlly Pramata, rachmapramata@gmail.com, Department of Biomedical Engineering, Telkom University, Purwokerto, Indonesia, Jl. D.I. Panjaitan No. 128, Purwokerto, 53147, Jawa Tengah, Indonesia.
DOI: https://doi.org/10.35882/jteknokes.v19i2.160

e-ISSN: 2407-8964
p-ISSN: 1907-7904

and the development of materials for electronic and communication applications. She is particularly focused on applying physical principles to understand material behavior at micro- and nano-scales, enabling innovations in material design for emerging technologies. Her work integrates concepts from condensed matter physics, electromagnetic theory, and material science to support advancements in modern electronic and communication systems.

Corresponding author: Rachma Cherlly Pramata, rachmapramata@gmail.com, Department of Biomedical Engineering, Telkom University, Purwokerto, Indonesia, Jl. D.I. Panjaitan No. 128, Purwokerto, 53147, Jawa Tengah, Indonesia.
DOI: https://doi.org/10.35882/jteknokes.v19i2.160